

# Mutual Coupling Compensation in Non-Uniform Antenna Arrays using Inter-Element Spacing Restrictions

F. Tokan and F. Gunes

Department of Electronics and Communication Engineering  
Faculty of Electrics and Electronics, Yıldız Technical University, Yıldız 34349, Istanbul, Turkey  
ftokan@yildiz.edu.tr, gunes@yildiz.edu.tr

**Abstract** — In the antenna array synthesis problems, most of the works in literature utilize isotropic elements. Thus, the mutual coupling effects between the array elements are neglected. It is obvious that an array antenna synthesized by neglecting the coupling effects cannot be used in the real world applications due to the possible incompatibilities between the desired and realized radiation patterns. In this work, two array antenna synthesis papers from literature are investigated in terms of mutual coupling effects so the necessary constraints are determined for the array geometry in order to compensate the coupling effects. Here, the same objectives of these two papers are achieved using the generalized pattern search (GPS) algorithm by considering the determined constraints for the inter-element spacings between the array elements. The resulted radiation patterns are validated with the computer simulation technology (CST) software with the aim of detecting possible incompatibilities due to the mutual coupling effects between the array elements. The simulation results verify that by using the constraints determined in this work, the radiation patterns obtained by pattern multiplication can provide the desired radiation demands also in the practical applications.

**Index Terms** — GPS algorithm, mutual coupling effects, non-uniform array, null control, sidelobe suppression.

## I. INTRODUCTION

Synthesis of linear antenna arrays has been extensively studied in the last 50 years [1-14]. Generally, the objectives in an array design are

achieving the minimum sidelobe level (SLL), maximization of the main beam in the desired direction and obtaining narrow or broad nulls in the directions of interfering signals. In most of the works realized in literature, the antennas of the array are accepted as isotropic. In these works, the possible mutual coupling effects between the array elements are neglected; thus, it is obvious that an array synthesized by neglecting the mutual coupling effects between the array elements may not be convenient for real world applications. Especially, in the works that the inter-element spacings between the elements are employed as optimization variables [4-8], the desired pattern and the pattern obtained in practical realization will not be in a good agreement. Besides, compensation of mutual coupling effects is also investigated in literature [11-12].

In this work, the full wave electromagnetic simulations (CST) of two works from literature [5-6] that have utilized isotropic elements and thus neglected mutual coupling effects between the array elements are performed to observe the differences between the desired and resulted patterns. Then, the reasons of the incongruity between the desired and resulted patterns are determined. Thus, the restrictions for the inter-elements spacings between the array elements are established to minimize the corruptions in the desired patterns occurred due to the mutual coupling effects.

Subsequently, in this work by using these restrictions, the same objectives of the examples in [5-6] are achieved using the GPS algorithm. The obtained array geometries can be used to obtain the desired radiation patterns also when they are used in the practical applications. The proposed

method can be efficiently employed in various antenna applications. Providing a simple approach by utilizing the determined inter-element spacing restrictions between the array elements, the synthesized radiation pattern will also be convenient for practical applications, thus there will be no need to perform electromagnetic simulation software to confirm the designed array geometry.

In this work, the GPS algorithm is used to achieve the same objectives that are used in [5-6]. GPS methods are introduced as an optimization tool into the antenna engineering for the array antenna synthesis. GPS are nonrandom methods for direct searching minima of a function which may even be discontinuous, non-differentiable, stochastic or highly nonlinear [15-20]. Moreover, the results of the GPS algorithm are validated by comparing with results obtained using the genetic algorithm (GA) and a full wave electromagnetic simulator (CST) which allows the prediction of the performance of antennas to very high accuracy without the need for costly trials and error constructions and measurements.

## II. PROBLEM FORMULATION

In the selected papers [5-6], the linear array antenna geometries with  $2N$  half-wave dipole antennas distributed symmetrically with respect to the origin along the  $y$ -axis is given in Fig. 1.

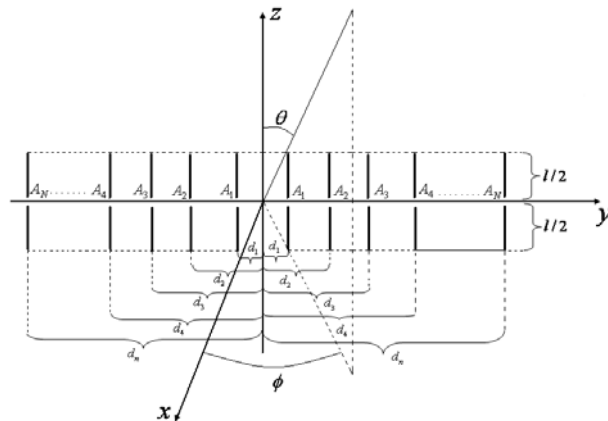


Fig. 1. The linear array antenna geometry with an even number of elements.

This linear array antenna has non-uniform inter-element spacings and also non-uniform excitations for array elements, thus the array factor

in the azimuth plane can be expressed as follows [21]:

$$AF = 2 \sum_{n=1}^N A_n \cos \left[ \frac{2\pi d_n}{\lambda} \sin \phi + \beta_n \right], \quad (1)$$

where  $2N$  is total number of the antenna elements,  $\lambda$  is the wavelength in free space;  $A_n$ ,  $\beta_n$  are the excitation amplitude and phase of the  $n$ th element, respectively and  $d_n$  is the distance from the origin to the  $n$ th element. In the papers we have used [5-6],  $\beta_n$  is fixed zero, thus the broadside arrays are worked out:

$$AF = 2 \sum_{n=1}^N A_n \cos \left[ \frac{2\pi d_n}{\lambda} \sin \phi \right]. \quad (2)$$

## III. GPS ALGORITHM

GPS methods are a class of direct search methods, originally introduced and analyzed by Torczon [15] for unconstrained minimization problems, and then extended by Lewis and Torczon to problems with bound [16] and general linear constraints [17]. GPS methods have been also adapted to solve nonlinearly constrained problems in an augmented Lagrangian framework [18]. A summary of the work on GPS methods can be found in [19]. Recently, a GPS method [20] is proposed to solve a class of non-smooth minimization problems, where the set of non-differentiability is included in the union of known hyper planes and, therefore, is highly structured. Both unconstrained and linearly constrained problems are considered.

GPS are the direct methods for searching minima of a function which may be even discontinuous, non-differentiable, stochastic, or highly nonlinear. Thus, they can be exploited efficiently in solving optimization problems without requiring any information about the gradient of the fitness function. As opposed to more traditional optimization methods that use information about the gradient or higher derivatives to search for an optimal point, a GPS algorithm searches a set of points around the current point, looking for one where the value of the fitness function is lower than the value at the current point.

It should be mentioned here that this paper is not intended to be an extensive review of GPS, and therefore only the main steps of the GPS algorithm we employed are explained here. The

reader is referred to [4, 15–20] and the references mentioned therein for a detailed discussion of the basic concepts of the GPS algorithm and how it works.

The GPS algorithm is applied to synthesize the same radiation pattern requirements of the selected papers. The objectives of these works are obtaining the minimum SLL and generating narrow or broad nulls in the directions of interfering signals. Thus, we have gathered these multiple objectives in a single fitness function as the logarithmic sums of the array factor,  $|AF(\phi)|$  given by (3) and (3.1) as follows:

$$\text{Fitness} = 20 \log \left\{ \sum \max \left\{ |AF(\phi)|_{\phi_u}^{\phi_l} \right\} \right\} + 20 \log \left\{ \sum_k |AF(\phi_k)| \right\},$$

(3)

subject to;

$$d_{n+1} - d_n \geq 0.5\lambda, \quad n = 1, \dots, N-1. \quad (3.1)$$

In (3),  $\phi_u$  and  $\phi_l$  are the upper and lower angles of the regions and  $\phi_k, k = 1, \dots, K$ , are the directions where the nulls are required. Equation (2) can be employed directly in (3). Thus, the first term in (3) is employed to minimize the SLL between the desired angles whereas the second one is for having zeros in the desired directions. (3.1) gives the constraint imposed on inter-element spacing to reduce mutual coupling effects between the elements of the array antennas.

#### IV. APPLICATION EXAMPLES

In this section, firstly the synthesized radiation patterns of the selected papers [5-6] are performed using a full wave electromagnetic simulator (CST) which allows the prediction of the performance of antennas to very high accuracy without the need for costly trial and error constructions and measurements. In both [5] and [6], the array elements are accepted as isotropic and the desired radiation patterns are synthesized by optimizing the positions of array elements. All of the simulations are realized using half-wave dipole antennas at 2.6 GHz.

Afterwards, the same objectives for the examples of literature are achieved again but this time, by using the determined constraints for the inter-element spacings. Thus, the mutual coupling

effects between antennas are minimized and the radiation patterns obtained using pattern multiplication can provide the desired radiation demands of practical applications. The results of the GPS algorithm are also validated by comparing with the results obtained using the GA for the same objective functions and restrictions. The GA is a stochastic algorithm that gives different solution sets after each run, thus the GA is run a few times with the same number of iterations of the GPS and the best results are given in this paper. The CST simulation results are also obtained for the recommended array geometries of the GPS algorithm with the aim of exhibiting the compatibility between the desired pattern and full-wave simulation result. Both the GPS and GA algorithms were implemented using MATLAB.

In [5], the authors have perturbed a -30 dB Dolph-Chebyshev initial pattern to form a null at  $20^\circ$  using a 20 isotropic element linear array. The mutual coupling effects are neglected in this example. The perturbation amounts, the resulted positions of each element and also the inter-element spacings of the adjacent elements are given in Table 1.

Table 1: The excitation amplitudes and the perturbed element positions for Fig. 2

|             |                 |   |
|-------------|-----------------|---|
| Dolph-Cheb. | $A_n(A)$        | 1.000 0.970 0.912 0.831 0.731 0.620 0.504 0.391 0.285 0.325               |
|             | $d_n(\lambda)$  | 0.250 0.750 1.250 1.750 2.250 2.750 3.250 3.750 4.250 4.750               |
|             | $d_{n+1} - d_n$ | 0.500 0.500 0.500 0.500 0.500 0.500 0.500 0.500 0.500 0.500               |
| [5]         | $A_n(A)$        | 1.000 0.970 0.912 0.831 0.731 0.620 0.504 0.391 0.285 0.325               |
|             | $d_n(\lambda)$  | 0.230 0.712 1.234 1.768 2.277 2.758 3.237 3.735 4.246 4.758               |
|             | $d_{n+1} - d_n$ | <b>0.460 0.482</b> 0.522 0.534 0.509 <b>0.481 0.479 0.498</b> 0.511 0.512 |

The radiation patterns which are symmetrical with respect to the origin are given before and after optimization processes in Fig. 2 together with the CST simulation pattern.

The optimized radiation pattern is obtained using the element positions given in Table 1. Although, the desired null direction seems to be suppressed in the optimized pattern, the CST simulation pattern of the optimized array proves that the desired direction can be suppressed only a few dB. Besides, an unexpected null level is formed directed to  $22^\circ$ . This amount of corruption in the expected null level and null direction is occurred because of the coupling effects between the array elements. Here, crucial differences are formed between the expected and occurred values

in the null deepness and null direction. When the element positions in Table 1 are observed, it can be seen that some of the spacings between the array elements are smaller than  $0.5\lambda$ .

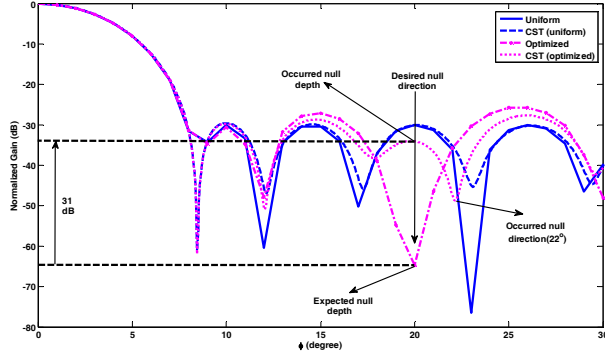


Fig. 2. Normalized radiation patterns obtained in [5] and the CST simulation pattern of the optimized array.

The spacing between the first elements about the origin is  $0.46\lambda$  where the spacings between the first and second elements, between the fifth and sixth elements and between the sixth and seventh elements are  $0.482\lambda$ ,  $0.481\lambda$ , and  $0.479\lambda$ , respectively. These values are given in bold style in Table 1.

In this paper, the same objectives of [5] are achieved by using the following cost function:

$$Fitness = 20 \log \left\{ \max_{\phi_l=8^\circ} \left\{ AF(\phi) \Big|_{\phi_u=90^\circ} \right\} \right\} + 20 \log \{ AF(20^\circ) \} \quad (4)$$

The GPS and GA algorithms are utilized to optimize (4), but this time using the determined restriction given with (3.1). The obtained solution spaces are given in Table 2 and the radiation pattern obtained using these solution spaces is given in Fig. 3.

Table 2: The excitation amplitudes and the perturbed element positions used to obtain Fig. 3

|             |                 |   |
|-------------|-----------------|---|
| GPS         | $A_n(A)$        | 0.250 0.750 1.250 1.787 2.338 2.838 3.338 3.838 4.338 4.990 |
|             | $d_n(\lambda)$  | 0.500 0.500 0.500 0.537 0.551 0.500 0.500 0.500 0.500 0.652 |
| GA          | $d_{n+1} - d_n$ | 0.264 0.779 1.283 1.840 2.382 2.884 3.389 3.897 4.419 5.079 |
|             | $A_n(A)$        | 0.528 0.515 0.504 0.557 0.542 0.502 0.505 0.508 0.522 0.660 |
| Dolph-Cheb. | $d_n(\lambda)$  | 0.250 0.750 1.250 1.750 2.250 2.750 3.250 3.750 4.250 4.750 |
|             | $d_{n+1} - d_n$ | 0.500 0.500 0.500 0.500 0.500 0.500 0.500 0.500 0.500 0.500 |

It can be observed from the resulted pattern of GPS optimizer that a very deep null is achieved successfully in the  $20^\circ$  direction. Although the

null level is also easily achieved using GA, the MSLL of GA pattern is slightly higher than the GPS pattern level in the desired null direction.

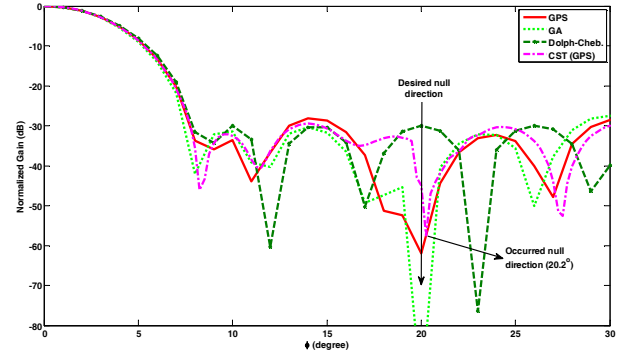


Fig. 3. Normalized radiation patterns optimized using the GPS and the GA algorithms with the CST simulation pattern of the optimized array.

As it is observed from Fig. 3, the resulted CST simulation pattern follows the features of the GPS pattern approximately in the all visible region. Besides, the CST simulation pattern has achieved a deep null level in the desired null direction which can be accepted as zero level for the practical applications.

In the second example [6], the authors have perturbed the positions of a 28 isotropic element array to achieve null levels at  $30^\circ$ ,  $32.5^\circ$ , and  $35^\circ$ . The mutual coupling effects are also neglected in this example. The perturbation amounts, the resulted positions of each element and also the inter-element spacings of the adjacent elements are given in Table 3.

Table 3: The excitation amplitudes and the perturbed element positions for Fig. 4

|          |                 |  |
|----------|-----------------|--|
| Uni-form | $A_n(A)$        | 1.000 1.000 1.000 1.000 1.000 1.000 1.000 1.000 1.000 1.000                      |
|          | $d_n(\lambda)$  | 0.250 0.750 1.250 1.750 2.250 2.750 3.250 3.750 4.250 4.750                      |
|          | $d_{n+1} - d_n$ | 0.500 0.500 0.500 0.537 0.551 0.500 0.500 0.500 0.500 0.652                      |
| [6]      | $A_n(A)$        | 1.000 1.000 1.000 1.000 1.000 1.000 1.000 1.000 1.000 1.000                      |
|          | $d_n(\lambda)$  | 0.280 0.780 1.220 1.750 2.270 2.740 3.265 3.770 4.195 4.750                      |
|          | $d_{n+1} - d_n$ | 0.560 0.500 <b>0.440</b> 0.530 0.520 <b>0.470</b> 0.525 0.505 <b>0.425</b> 0.555 |

The radiation patterns before and after the optimization process are given in Fig. 4 together with the CST simulation patterns. The optimized radiation pattern is obtained using the array geometry given in Table 3. The desired null directions are achieved in [6] by using isotropic

elements, thus by neglecting the mutual coupling effects. The CST simulation pattern shows that the expected and occurred null levels are quite different as illustrated in Fig. 4.

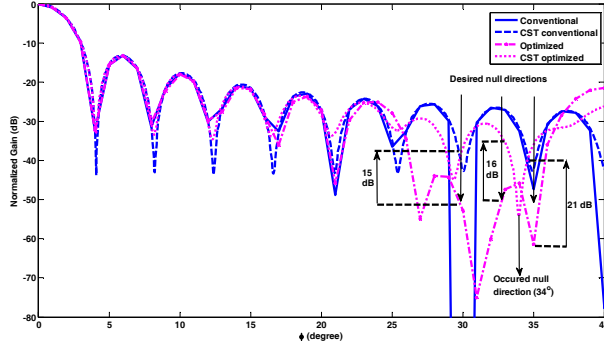


Fig. 4. Normalized radiation patterns obtained in [6] and the CST simulation pattern of the optimized array.

An only null level is formed directed to  $34^\circ$  rather than the expected three null directions. It is obvious that this array geometry cannot be used in a real world problem to obtain nulls in the desired directions. When the element positions in Table 3 are investigated, it can also be seen that many of the spacings between the elements are smaller than  $0.5\lambda$ . The first and second elements is  $0.44\lambda$ , between the fifth and sixth elements is  $0.47\lambda$ , between the eighth and ninth elements is  $0.425\lambda$ , between the eleventh and twelfth elements is  $0.395\lambda$ , and between the twelfth and thirteenth elements is  $0.45\lambda$ . These values are given in bold style in Table 3.

In the second implementation, the following cost function is arranged to achieve the same objectives of [6]:

$$\begin{aligned} \text{Fitness} = & 20 \log \{ AF(30^\circ) \} + 20 \log \{ AF(32.5^\circ) \} \\ & + 20 \log \{ AF(35^\circ) \} + 20 \log \left\{ \max \left\{ \left| AF(\varphi) \right|_{\varphi_i=90^\circ}^{\varphi_i=4^\circ} \right\} \right\}. \end{aligned} \quad (5)$$

The cost function is optimized using both the GPS and GA algorithms but this time with the determined restrictions in (3.1). The optimized element positions are given in Table 4 and the radiation pattern obtained using these element positions is given in Fig. 5.

It is obvious from Fig. 5 that the null levels and directions are easily achieved with both GPS and GA algorithms. Besides, the close-in sidelobes

are almost the same for both the GPS and the GA, but the far sidelobes are better for the GPS. As it is observed from Fig. 5, the resulted CST simulation pattern follows the features of the GPS pattern in the close-in sidelobes and the maximum level of  $-40$  dB is occurred in the desired null directions. It can be said that, by our improvements in this paper, the disagreement between the desired pattern and the CST simulation pattern can be prevented, thus the obtained array geometries can achieve the desired radiation patterns also when used in practical applications.

Table 4: The excitation amplitudes and the perturbed element positions used to obtain Fig. 5

|             |                 |  |
|-------------|-----------------|--|
| GPS         | $d_n(\lambda)$  | 0.250 0.750 1.311 1.811 2.311 2.811 3.461 3.962 4.461 4.961<br>5.772 6.272 6.772 7.273 |
|             | $d_{n+1} - d_n$ | 0.500 0.500 0.566 0.500 0.500 0.500 0.650 0.501 0.499 0.500<br>0.811 0.500 0.500 0.501 |
| GA          | $d_n(\lambda)$  | 0.252 0.752 1.251 1.754 2.257 2.756 3.284 3.792 4.291 4.790<br>5.463 5.965 6.465 7.094 |
|             | $d_{n+1} - d_n$ | 0.504 0.500 0.499 0.503 0.503 0.499 0.528 0.508 0.499 0.499<br>0.673 0.502 0.500 0.629 |
| Dolph-Cheb. | $d_n(\lambda)$  | 0.266 0.800 1.333 1.866 2.400 2.933 3.466 4.000 4.533 5.066<br>5.600 6.133 6.666 7.200 |
|             | $d_{n+1} - d_n$ | 0.532 0.534 0.533 0.533 0.534 0.533 0.533 0.534 0.533 0.533<br>0.534 0.533 0.533 0.534 |

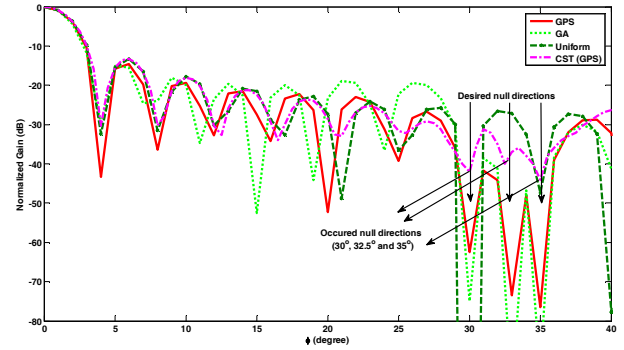


Fig. 5. Normalized radiation patterns optimized using the GPS and the GA algorithms with the CST simulation pattern of the optimized array.

## VI. CONCLUSION

This paper illustrated the corruptions in the desired radiation patterns of non-uniform antenna arrays due to the mutual coupling effects between the array elements. Two examples from literature are utilized to demonstrate the disagreement between the desired and occurred radiation patterns. In our paper, it is confirmed that a non-uniform array geometry synthesized by neglecting the coupling effects cannot be used in real world applications.

We have achieved the same objectives of the selected papers with the determined inter-element spacing restrictions (3.1) using the GPS algorithm.

The GPS is a direct, efficient derivative-free algorithm for searching minima of the functions. By our improvements in this paper, we prevent the disagreement between desired pattern and the resulted pattern using the necessary restrictions for the inter-element spacings. Thus, the radiation patterns obtained using pattern multiplication can provide the desired radiation demands of practical applications. The verification of this approach is carried out by comparing the results of CST software.

### REFERENCES

- [1] K. K. Yan and Y. L. Lu, "Sidelobe Reduction in Array Pattern Synthesis using Genetic Algorithm," *IEEE Trans. Antennas Propagat.*, vol. 45, pp. 1117–1122, 1997.
- [2] G. K. Mahanti, N. Pathak, and P. Mahanti, "Synthesis of Thinned Linear Antenna Arrays with Fixed Sidelobe Level Using Real-Coded Genetic Algorithm," *Progress In Electromagnetics Research*, vol. 75, pp. 319–328, 2007.
- [3] G. K. Mahanti, A. Chakrabarty, and S. Das, "Phase-Only and Amplitude-Phase Only Synthesis of Dual-Beam Pattern Linear Antenna Arrays Using Floating-Point Genetic Algorithms," *Progress In Electromagnetics Research*, vol. 68, pp. 247–259, 2007.
- [4] F. Gunes and F. Tokan, "Pattern Search Optimization with Applications on Synthesis of Linear Antenna Arrays," *Expert Systems with Applications*, vol. 37, pp. 4698–4705, 2010.
- [5] T. H. Ismail and M. M. Dawoud, "Null Steering in Phased Arrays by Controlling the Element Positions," *IEEE Transactions on Antennas and Propagat*, vol. 39, pp. 1561–1566, 1991.
- [6] M. M. Khodier and C. G. Christodoulou, "Linear Array Geometry Synthesis with Minimum Sidelobe Level and Null Control Using Particle Swarm Optimization," *IEEE Transactions on Antennas and Propagat.*, vol. 53, pp. 2674–2679, 2005.
- [7] V. Murino, A. Trucco, and C. S. Regazzoni, "Synthesis of Unequally Spaced Arrays by Simulated Annealing," *IEEE Transactions on Signal Processing*, vol. 44, pp. 119–127, 1996.
- [8] D. W. Boeringer and D. H. Werner, "Particle Swarm Optimization Versus Genetic Algorithms for Phased Array Synthesis," *IEEE Transactions on Antennas and Propagat.*, vol. 52, pp. 771–779, 2004.
- [9] K. R. Mahmoud, M. I. Eladawy, R. Bansal, S. H. Zainud-Deen, and S. M. M. Ibrahim, "Analysis of Uniform Circular Arrays for Adaptive Beamforming Applications Using Particle Swarm Optimization Algorithm," *International Journal of RF and Microwave Computer-Aided Engineering*, vol. 18, pp. 42–52, 2008.
- [10] K. Guney, B. Babayigit, and A. Akdagli, "Interference Suppression of Linear Antenna Arrays by Phase-Only Control Using a Clonal Selection Algorithm," *Journal of the Franklin Institute*, vol. 345, pp. 254–266, 2008.
- [11] W. Choi, T. K. Sarkar, O. Allen, and J. Asvestas, "Approximate Compensation for Mutual Coupling in a Direct Data Domain Least Squares Approach using the In-situ Measured Element Patterns," *Applied Computational Electromagnetic Society (ACES) Journal*, vol. 21, no. 3, pp. 342–352, 2006.
- [12] V. N. S. Kalaga and M. Hamid, "On The Optimum Directivity of Dipole Arrays Considering Mutual Coupling," *Applied Computational Electromagnetic Society (ACES) Journal*, vol. 23, no. 2, pp. 155–165, 2008.
- [13] F. Hutu, S. Cauet, and P. Coirault, "Robust Synchronization of Different Coupled Oscillators: Application to Antenna Arrays," *Journal of the Franklin Institute*, vol. 346, pp. 413–430, 2009.
- [14] K. Guney and A. Akdağlı, "Null Steering of Linear Antenna Arrays Using a Modified Tabu Search Algorithm," *Progress In Electromagnetics Research*, vol. 33, pp. 167–182, 2001.
- [15] V. Torczon, "On the Convergence of Pattern Search Algorithms," *SIAM Journal on Optimization*, vol. 7, pp. 1–25, 1997.
- [16] R. M. Lewis and V. Torczon, "Pattern Search Algorithms for Bound Constrained Minimization," *SIAM Journal on Optimization*, vol. 9, pp. 1082–1099, 1999.
- [17] R. M. Lewis and V. Torczon, "Pattern Search Methods for Linearly Constrained Minimization," *SIAM Journal on Optimization*, vol. 10, pp. 917–941, 2000.

- [18] R. M. Lewis and V. Torczon, "A Globally Convergent Augmented Lagrangian Pattern Search Algorithm for Optimization with General Constraints and Simple Bounds," *SIAM Journal on Optimization*, vol. 12, pp. 1075–1089, 2002.
- [19] T. G. Kolda, R. M. Lewis, and V. Torczon, "Optimization by Direct Search: New Perspectives on Some Classical and Modern Methods," *SIAM Rev.*, vol. 45, pp. 385–482, 2003.
- [20] C. Bogani, M. G. Gasparo, and A. Papini, "Generalized Pattern Search Methods for a Class of Nonsmooth Optimization Problems with Structure," *Journal of Computational and Applied Mathematics*, vol. 229, pp. 283–293, 2009.
- [21] R. S. Elliott, *Antenna Theory and Design*, Prentice-Hall, 1981.



**Fikret Tokan** received the M.S. degree in Electronics and Communications Engineering from the Yıldız Technical University in 2005 and Ph.D. degree from the Yıldız Technical University, Istanbul, in Communications Engineering in 2010.

He has been currently working as a researcher in Yıldız Technical University. His current research interests are electromagnetic waves, propagation, antenna arrays, scattering, and numerical methods.



**Filiz Güneş** received her MSc degree in electronic and communication engineering from the Istanbul Technical University. She attained her PhD degree in communication engineering from the Bradford University in 1979.

She is currently a full professor in Yıldız Technical University. Her current research interests are in the areas of multivariable network theory, device modeling, computer-aided microwave circuit design, monolithic microwave integrated circuits, and antenna arrays.